Biomass Conversion and Biorefinery (2022) 12:4127–4137
https://doi.org/10.1007/s13399-020-01216-9

ORIGINAL ARTICLE

Bioremoval of Safranin O dye by the identified lichen species called *Evernia prunastri* biomass; biosorption optimization, isotherms, kinetics, and thermodynamics

Zeynep Mine Şenol[1] · Ülküye Dudu Gül[2] · Selçuk Şimşek[3]

Received: 23 September 2020 / Revised: 1 December 2020 / Accepted: 14 December 2020 / Published online: 6 January 2021

Abstract

Evernia prunastri (lichen), a novel, eco-friendly, cost-effective, wide availability, safe, renewable and easy collection biosorbent, has been utilized for the removal of Safranin O (SO) dye from an aqueous solution. The biosorption behavior of SO onto the lichen biomass was investigated concerning parameters such as initial SO concentration (10–2000 mg L^{-1}), solution pH (2.0–12.0), lichen biomass dosage (1–20 g L^{-1}), contact time (2–1440 min), temperature (5 °C, 25 °C, and 40 °C), and recovery were investigated. The zeta potential analyses showed that electrostatic attraction existed during the biosorption process between the SO and lichen biomass. The maximum SO biosorption capacity of the lichen biomass was 0.257 mol kg^{-1} at pH 6.0 and 25 °C. The biosorption energy for SO onto the lichen biomass was found to be E_{DR}:8.9 kJ mol^{-1} reveals the biosorption proceeds chemically. The biosorption process follows the pseudo-second order and intra particle diffusion rate kinetics. Thermodynamic studies showed that SO biosorption, by this the lichen biomass is possible, spontaneous, and endothermic.

Keywords Lichen · *Evernia prunastri* · Biosorption · Cationic dye · Safranin O

1 Introduction

The organisms called lichens are compose of symbiotic association of fungi and algae or cyanobacteria [1]. Fungi and algae or cyanobacteria are respectively called as mycobiont and photobiont in the association. The role of mycobiont is to protect the organism and, also functions as an inorganic food reservoir of the organism [2]. On the other hand, the photobiont ensures the glikoz production with photosenthesis for the nutritional and energy needs of organism [3]. It is known that in the association-forming lichen organism, both the mycobiont and photobiont benefit from each other [4]. Also, the formed lichen organism has more tolerant of adverse conditions. However, the identification of lichen species is also very complicated because lichens are composed of two different organisms [5]. Recently, besides morphological identification, DNA-based identification has been used to identify lichens [6]. In addition, the various lichen acids produced by lichen species can be used in the identification of lichen species [7]. Identification of the lichen species, providing to learn lichen properties, is an important issue due to determine their usability in variety of industrial areas.

Most of the recent studies focus on the utilization of the lichen species as low-cost and easily available biosorbents in wasrewater treatment [8–10]. However, there is limited information about the mechanism of biosorption process by lichen biosorbents. Lichen acids' characteristic of lichen type are found on the surface of Lichens. These are the structures on the lichen surface of the parts where the adsorbate in the environment interacts during the biosorption process. These lichen acids found in lichen thalli are polymers composed of polysaccharides. The lichen acids found in the *Evernia prunastri* thalli take the name Eveniin and consist of glucans containing α (1 → 3) (1 → 4) linkages [11].

✉ Zeynep Mine Şenol
msenol@cumhuriyet.edu.tr

[1] Department of Food Technology, Zara Vocational School, Cumhuriyet University, 58140 Sivas, Turkey

[2] Biotechnology Application and Research Center, Vocational School of Health Services, Bilecik Seyh Edebali University, 11230 Bilecik, Turkey

[3] Department of Chemistry, Faculty of Science, Cumhuriyet University, 58140 Sivas, Turkey

Dyes are commonly used in different industrial areas, and the wastewaters of these industrial areas contain large amount of dangerous dyes. For instance, Safranin O (SO) dye extensively used as colorant in some industries such as painting and paper [12, 13]. In addition to this, SO is a highly water soluble dye which means that SO is found at high concentrations in the wastewaters [12]. It was reported that this dye was toxic, allergenic, or carcinogenic at higher concentrations in aquatic environments [13]. It is essential to remove the dyes and their breakdown pollutants from wastewaters to protect the living organisms and environment [14, 15]. So, it is required to treat the wastewaters containing large amount of dyes such as SO before discharging from the end industrial applications [16].

Adsorption is recommended as a useful process for the treatment of industrial effluents [17, 18]. Particularly, the removal of dyes, which are toxic and carcinogenic for the living organisms, from aquatic environments has been successfully realized by adsorption process [19, 20]. To reduce the cost of this process, most of the latest studies search to find low-cost adsorbents [21–23]. Recent studies reported that the biological materials are recommended low-cost adsorbents for the treatment of dyeing wastewaters [24]. The recent studies showed that lichen species were both effective and efficient biosorbents for removal of heavy metals from aquoeus solutions [8, 10]. Also, Bayazit et al. [25] showed that the lichen species called *Cladonia convoluta* (Bilecik, Turkey) performed successful textile dye (Acid Red) removal with the inexpensive and ecofriendly nature. The aim of this study is to determine the SO biosorption properties of a lichen biomass collected from Bilecik, Turkey and obtain detailed information about the mechanism of dye biosorption process. Also to our own knowledge, there is not any study showing the removal of Safranin O dye by the lichen species identified as *Evernia prunastri* obtained from Bilecik, Turkey province.

2 Materials and methods

2.1 Materials

The Safranin O dye was obtained from (Sigma-Aldrich, Germany) as pure form and used in the biosorption experiments. The phsicochemical properties of SO was given in Table 1. Other chemicals used in this study were purchased from Merk (Germany).

2.2 FT-IR, SEM-EDX, and BET analyses

FT-IR spectra of unloaded and SO-loaded lichen biomass were recorded in a Perkin Elmer 400 spectro-photometer. The surface of unloaded and SO-loaded lichen biomass was characterized by FT-IR, SEM-EDX, and BET analyses. SEM equipped with an energy dispersive spectrometer (EDX) attachment images of unloaded and SO-loaded lichen biomass were obtained with a Leo 440 Computer Controlled Digital System.

The specific surface area and micropore volume of lichen biosorbent in the absence and presence of SO were measured using N_2 adsorption-desorption (AUTOSORB 1C) at − 196 °C. The surface area, total pore volume, and micropore volume were determined by multipoint BET (Brunauer, Emmett, and Teller), *t* plot, and D-R (Dubinin–Radushkevic), respectively [26].

2.3 Biomass preparation

The morphologically detected lichen biomasses were collected from the bark of oak trees in the urban forest of Bilecik province (N 400 11.5262′, E 0290 57.962′) in Turkey. The lichen samples were cleaned of macroimpurities, washed with double-distilled water and air-dried at room temperature for 72 h. The dried samples were cleaned meticulously with plastic tweezers for removing the possible materials (the oak bark and soil particles) under binocular microscope (Primo Star Zeiss) and finally powdered and sieved.

2.4 Molecular identification of lichen sample

Qiagen Blood & Tissue isolation kit was used for DNA isolation. In PCR, experiments were carried out in a reaction solution with a volume of 50 uL including 10× Taq buffer (Thermo) (5 uL), 25 mM MgCl (3 uL), 2 mM dNTP mixture (5 uL), 20 pmol for each primer (1 uL), 0.5 U uL^{-1} Taq polymerase (Thermo) (0.3 uL), and 150 ng of DNA were used. The BioRad T100 model PCR machine was used. PCR conditions are listed as waiting 5 min at 94 °C and 30 cycles (30 s at 94 °C + 30 s at 50 °C + 45 s at 72 °C in one cycle). The primers used in this study are given in Table 2.

Nucleospin Gel and PCR Cleanup Kit were used for PCR purification. Bigdye Cycle Sequencing Kit v3.1 and ABI 3100 Genetic Analyzer were used for DNA sequence analysis. In post-sequence purification experiments; the method as outlined in the manual was done using the Bigdye kit was made by NaOAc-Ethanol precipitation.

2.5 Biosorption experiments

The biosorption of SO onto lichen biomass was investigated by using the batch method. Stock SO solution containing 1000 mg L^{-1} of dye was prepared using double-distilled water. All experiments were carried out at a shaking rate of 150 rpm in 10-mL polypropylene tubes containing 100 mg lichen biomass at constant concentration of 500 mg L^{-1} SO in 10 ml solutions. The all biosorption studies of SO were performed in their natural pHs (6.0) except the study of effect of pH on biosorption. The pH was adjusted with dilute HCl and

Table 1 The physical and chemical properties of SO dye

Color and structure	Reddish brown powder
Ionic structure	Cationic (having imine group)
Water solubility	Highly soluble
Maximum wave length (nm)	520
Molecular formula	$C_{20}H_{19}N_4Cl$
Molecular weight (g mol^{-1})	350.85
IUPAC name	3,7-Diamino-2,8-dimethyl-5-phenylphenazinium chloride
Generic name	C.I. basic red 2
Molecular structure	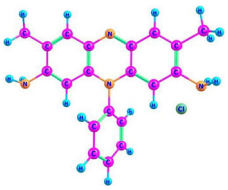

NaOH. The details of experimental conditions were explained in Table 3 for all biosorption assays in this study. The concentrations of SO in solutions were determined spectrophotometrically by measuring the absorbance of the solutions at 520 nm [27]. The SO concentrations were determined with a UV-visible spectrophotometer (Shimadzu, 160 A model, Kyoto, Japan). All experiments were done in duplicate and the double-distilled water was used in all experiments. Eq. 1 and Eq. 2. were used to calculate biosorption % and Q (mol kg^{-1}).

$$\%\text{Biosorption} = \left[\frac{C_i - C_f}{C_i}\right] \times 100 \tag{1}$$

$$Q = \left[\frac{(C_i - C_e)V}{m}\right] Q = \left[\frac{(C_i - C_e)V}{m}\right] \tag{2}$$

where, Q is the amount of SO dye adsorbed per gram of adsorbent at any time (mol kg^{-1}); C_i and C_f are the initial and equilibrium concentration of SO dye (mg L^{-1}) in the solution; m refers to the biosorbent mass (g) and V is the solution volume (L).

2.6 Desorption experiments

Batch systems were used in the desorption processes in order to evaluate the re-use efficiency. The lichen biomass (100 mg) was added to polypropylene tubes containing 10 mL HCl, NaOH, and ethyl alcohol (each one, 0.1 mol L^{-1}) solutions and at a shaking rate of 150 rpm for 24 h. The solutions were centrifuged at 5000 rpm for 10 min, and the supernatant concentration was subsequently measured by UV-vis spectrophotometric method. Percent desorption was calculated with Eq. 3.

$$\text{Desorption}\% = \frac{Q_{\text{des}}}{Q_{\text{ads}}} \times 100 \tag{3}$$

In this equation, Q_{des} is the desorbed amount of SO (mol kg^{-1}); Q_{ads} is the biosorbed amount of SO (mol kg^{-1}).

Table 2 The used primers

ITS1	TCCGTAGGTGAACCTGCGG	White et al. 1990
ITS4	TCCTCCGCTTATTG ATATGC	White et al. 1990

2.7 The calculation of biosorption isotherms, kinetics, and thermodynamics

The biosorption isotherms is very useful to describe the interaction and the equilibrium between the biosorbate and the biosorbent. Three isotherm models, Langmuir, Freundlich, and Dubinin Radushkevich (D-R) isotherm models were used to specify the biosorption process, surface properties, and biosorption mechanism of the lichen biosorbent. The Langmuir model accepts the surface homogeneous, which is the most suitable model for determining the maximum monolayer capacity of the adsorbent. D-R model is used for more precise results for adsorption energy. Freundlich isotherm gives the most accurate information about surface heterogeneity [28–31]. The Langmuir, Freundlich, and D-R isotherm equations are expressed by the following (Eq. 4, Eq. 5, and Eq. 6, respectively)

$$Q = \frac{X_L K_L C_e}{1 + K_L C_e} \tag{4}$$

$$Q = K_F C_e^{\beta} \tag{5}$$

$$Q = Q_{\text{DR}} e^{-K_{\text{DR}}\varepsilon^2} \tag{6}$$

Table 3 Batch experimental conditions for biosorption of SO onto lichen

Aim of experiment	Solution pH	Biosorbent dosage (g L^{-1})	Inital SO conc. (mg L^{-1})	Contact time (min)	Temperature (°C)
Effect of pH	1.0–12.0	100	500	1440	25
Biosorbent dosage	6.0	10–200	500	1440	25
Effect of concentration	6.0	100	10–2000	1440	25
Effect of time	6.0	300	500	2–1440	25
Effect of temperature	6.0	100	500	1440	5, 25, 40
Desorption	6.0	100	500	1440	25

where, Q (mol kg^{-1}) is the amount of biosorbed SO, K_L is the parameter for Langmuir isotherm, and C_e is the equilibrium concentration (mol L^{-1}). K_F: Freundlich constant, β: biosorbent surface heterogeneity, and X_L is the maximum biosorption capacity. X_{DR} is a measure of biosorption capacity; K_{DR} is the activity coefficient (mol^2KJ^2) and ε is the Polanyi potential, R is the ideal gas constant (8.314 $Jmol^{-1}$ K^{-1}) and T is the absolute temperature (K). The Polanyi potential (ε) is expressed by the following Eq. 7:

$$\varepsilon = RTln\left(1+\frac{1}{C_e}\right) \tag{7}$$

The biosorption energy (E) is expressed by the following Eq. 8:

$$E_{DR} = (2K_{DR})^{-0.5} \tag{8}$$

The E indicates the biosorption mechanism, physical, or chemical. If the biosorption energy is $8 < E < 16$ kJ mol^{-1}, the biosorption is chemically controlled, and $E < 8$ $kJmol^{-1}$ indicates that the biosorption proceeds physically [32].

One of the important parameters of the biosorption process is to know the contact time. Prediction of the completion time of biosorption is main both for the kinetic control of the process and renewal of the biosorbent. The determination of the rate of biosorption and the rate of biosorption velocity will be possible only by investigating the compatibility of experimental results to different kinetic models. The kinetic models used in biosorption studies and applied to description the biosorption kinetics such as the pseudo-first order (PFO) [22], pseudo-second order (PSO), and intra particle diffusion (IPD) kinetic models [23] were used in this study, the equations (Eq. 9, Eq. 10 and Eq. 11, respectively)

$$Q_t = Q_e\left[1-e^{-k_1 t}\right] \tag{9}$$

$$Q_t = \frac{t}{\left[\frac{1}{k_2 Q_e^2}\right] + \left[\frac{t}{Q_e}\right]} \tag{10}$$

$$Q_t = k_i t^{0.5} \tag{11}$$

where, Q_t (mol kg^{-1}) is the biosorbed amount at time t (min); Q_e (mol kg^{-1}) is the biosorbed amount at equilibrium; k_1, k_2, and k_i is the rate constant of the PFO (min^{-1}), the PSO model (mol^{-1} kg min^{-1}), and the intra IPD (mol^{-1} kg $min^{-0.5}$) model, respectively.

Thermodynamic parameters of biosorption are very important to explain the effect of the temperature on the SO biosorption on lichen biomass. Enthalpy and entropy (ΔH^0 and ΔS^0) are obtained from $\ln K_D$ against 1/T, the graph. The slope ($-\Delta H^0/R$) and y- intercept ($\Delta S^0/R$) of the data plotted as $\ln K_D$ against $1/T$ the graph [33]. The Gibbs free energy (ΔG^0) is calculated from Eq. 15. ΔH^0, ΔS^0, and ΔG^0 were calculated using the following equations:

$$K_D = \frac{Q}{C_e} \tag{12}$$

$$\Delta G = -\mathrm{RT}lnK_D \tag{13}$$

$$lnK_D = \frac{\Delta S^0}{R} - \frac{\Delta H^0}{\mathrm{RT}} \tag{14}$$

$$\Delta G^0 = \Delta H^0 - T\Delta S^0 \tag{15}$$

3 Results and discussion

3.1 Molecular identification and properties of the lichen sample

The results of molecular identification analysis showed that the name of the lichen species was *Evernia prunastri*. *Evernia prunastri* is also known as "oakmoss" due to its habitat named oak tree [34]. It was reported that the cell wall of the lichen thalli contained large amount of polysaccharides [35], and these molecules were the first barriers that the adsorbate interacts. It was considered that these polysaccharides are responsible for the adsorption sites of the lichen biosorbents. The name of the polysaccharide in the *Evernia prunastri* was a

cold water-soluble lichenan-type of b-glucan from a linkage ratio of 3:1 with the (1 → 3) and (1 → 4) linkage dominating [36]. Also another isolichenin called Everniin was investigated in *Evernia prunastri*, and the structure of this polysaccharide was an alfa-polyglucan containing (1 → 3) and (1 → 4) linkage in the ratio of 4:1 [36].

3.2 Effect of inital pH and PZC for lichen

One of the most important factors affecting biosorption is solution pH [37]. In all biosorption experiments, the removal of the cationic dye SO has been studied in its own solution pH. Natural pH of 500 mgL^{-1} of cationic dye SO was measured as pH:6.0. Different pH values (2, 4, 6, 8, 10, and 12) were studied to explain the effect of pH on biosorption (Fig. 1). The obtained results are presented in Fig. 1. The obtained results presents a minimum at pH:2.0 and increases up to pH:6.0, then remains nearly constant over the initial pH:6.0–10.0 ranges and increases at pH:10.0–12.0 ranges. At low pHs, the lichen surface was protonated and, the cationic dye SO competed effectively with the H^+ ions. So, the amount of SO removal was decreased. At high pHs, the H^+ ions concentration decreased and the amount of SO removal was increased [27]. This inference can be further supported by the point of zero charge (PZC) value of the lichen. To better understand the biosorption mechanism, it is necessary to determine the PZC of the lichen biomass. To determine the PZC, 100 mg of lichen sample was added to polypropylene tubes containing 10 mL of KNO_3 solution (0.1 M), and the initial pH was adjusted to be between 2 to 12 using HCl and NaOH solutions (each one, 0.1 and/or 1.0 mol L^{-1}). The polypropylene tubes were sealed and shaken vigorously for 24 h. And then, the equilibrium pH values were measured. The results are given in Fig. 1. The value of pH_{pzc} of lichen biomass was as 4.53, which falls in the acidic region. At low pHs, the surface charge of lichen biomass is positive at pH < 4.53, and H^+ ions and cationic dye SO compete for biosorption to active centers of lichen biomass. As a result, cationic dye SO biosorption is decreased. At high pHs, the surface charge of lichen biomass is negative at pH > 4.53, and OH^- ions and cationic dye SO compete for biosorption to active centers. As a result, biosorption of cationic dye SO is increased [38]. It has been believed that cationic dye SO at natural pH 6.0 is biosorbed onto the surface of biosorbent by pH sensitive electrostatic interactions.

3.3 Effect of biosorbent dosage

According to Fig. 2, with increase in the lichen biomass amount, the SO removal of the dye increased remarkably. The results given in Fig. 2 showed that the SO removal efficiency increased with the amount of the lichen biomass increased due to the increase in active centers on the lichen surface. Thus, cationic dye SO penetrated more with ease into the biosorption sites. The maximum biosorption was found to be approximately 97% in the amount of 20 g L^{-1} the lichen biomass, as the number of biosorption active binding centers increased due to the increase in the dosage of the lichen biomass. The increase of SO removal is owing to the availability of active binding centers for biosorption [39]. The increasing biosorbent dosage caused an increment of biosorption rate due to the increased active binding centers for biosorption of cationic dye SO.

3.4 Biosorption isotherm models

The biosorption isotherms of the lichen biomass for SO were shown in Fig. 3. The biosorption isotherm constants for SO biosorption were presented in Table 4. The biosorption of SO increased with increasing SO concentration. It was observed that, when the nonlinear regression coefficient (R^2) which, obtained Langmuir and Freundlich isotherms were compared,

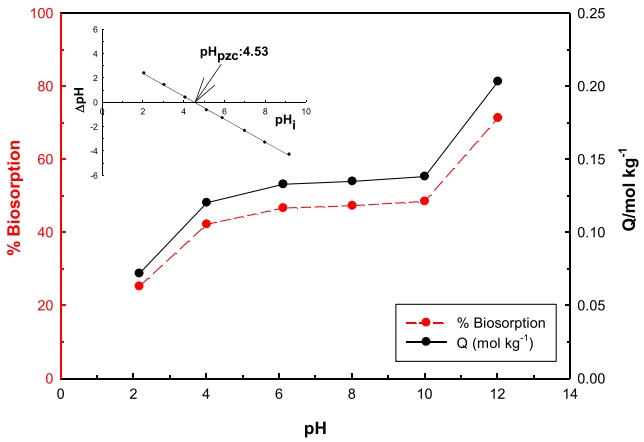

Fig. 1 Effect of pH on biosorption of SO onto lichen ([SO]$_0$:500 mg L^{-1}, biosorbent dosage:100 mg, V:10 mL, pH:2.0–12.0, contact time:1440 min, temperature: 25 °C) and PZC plots of lichen

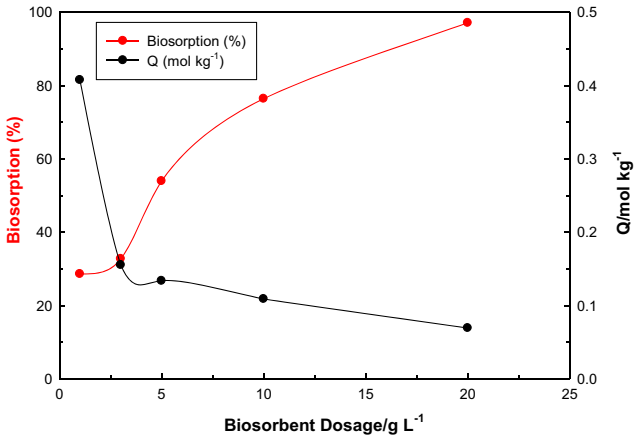

Fig. 2 Effect of biosorbent dosage on biosorption of SO onto lichen ([SO]$_0$:500 mg L^{-1}, biosorbent dosage:10, 30, 50, 100, 200 mg, V:10 mL, pH:6.0, contact time:1440 min, temperature: 25 °C)

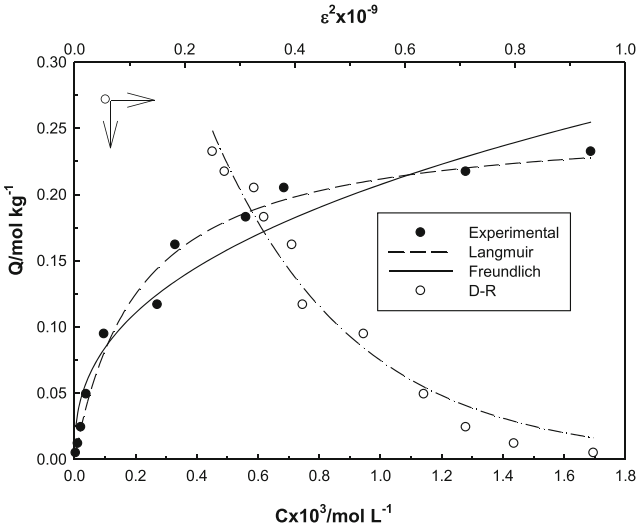

Fig. 3 Biosorption isotherm models ($[SO]_0$:10–2000 mg L^{-1}, biosorbent dosage:100 mg, V:10 mL, pH:6.0, contact time:1440 min, temperature: 25 °C)

the Langmuir isotherm model ($R^2 = 0.984$) was suitable for defining the biosorption of SO onto lichen biomass. The monolayer biosorption capacity of the lichen biosorbent for SO was 0.257 mol kg^{-1}. The SO biosorption results of the lichen biomass showed that the lichen biomass has a very high biosorption capacity. The K_L value was found in 4729 $Lmol^{-1}$. The K_F biosorption capacity was found 3.09, and β surface heterogeneity was also found as 0.391; both were obtained from the Freundlich model. Since the β value was between 0 and 1, the biosorption of SO onto lichen biomass was favorable. The Freundlich parameter β indicates the degree of heterogeneity of the surface, and the E_{DR} value found in the DR model indicates that the biosorption is chemical.

The reported studies about the SO biosorption properties of the various adsorbents were presented in Table 5. Among the biosorption capacities for SO of the different adsorbents reported in the literature, the lichen species used in this study called *Evernia prunastri* performed the most successful SO removal capacity from aqueous solutions under the determined optimal conditions.

Table 4 Langmuir, Freundlich, and Dubinin-Radushkevich isotherm models parameters

Isotherm	Parameter	Value	R^2
Langmuir	X_L (mol kg^{-1})	0.257	0.984
	K_L (L mol^{-1})	4729	
Freundlich	K_F	3.09	0.946
	β	0.391	
D-R	X_{DR} (mol kg^{-1})	0.666	0.968
	$K_{DR}x10^9/mol^2KJ^{-2}$	3.94	
	E_{DR}/kJ mol^{-1}	8.90	

3.5 Biosorption kinetics

The biosorption kinetics are very important to design the biosorption process. Biosorption kinetics give information about how long the biosorption is completed, the speed of the biosorption and the mass transfer mechanism. The binding of dye molecules in the biosorption process involves different mechanisms [48]. The following are the three consecutive steps that take place during the biosorption process of SO dye onto the lichen biomass surface: (i) transport of SO dye molecules from the bulk solution to the external surface of the lichen biomass (external diffusion), (ii) transport of SO dye molecules into the pores of the lichen biomass, excluding the small amount of biosorption occurring at the external surface of the biosorbent (particle diffusion or internal diffusion) and (iii) biosorption of the SO dye molecules on the interior surface of the lichen biomass (biosorption) [49].

The effect of contact time on the biosorption of SO is presented in Fig. 4. The biosorption increased with an increase in contact time. The SO removal is rapid at the initial stages of biosorption at different initial concentrations. By increasing contact time, the biosorption gradually decreased until reaching equilibrium. When the Fig. 4 examined, it was observed that biosorption reached equilibrium within 240 min (4 h). The correlation coefficients, which are a measure of the harmony of adsorption to kinetic models, are used to determine the appropriate model. When the correlation coefficients of the PFO and PSO kinetic models were compared, it was seen that the biosorption kinetics was better fit with the PSO kinetic model. At the same time, when the experimentally calculated Q_t values and the theoretically calculated Q_e values were examined (Table 6), the results of the PSO kinetic model were found to be closer to each other. The biosorption kinetics showed that the biosorption process better adapted to PSO kinetic. The PSO model predicts the rate of biosorption through a mass transfer with low initial concentrations. However, in the biosorption process, it plays an active role in diffusion into the particle. The IPD model assumes that diffusion is the determining step to control the biosorption rate. Also, the IPD has two linear components, that the adsorption process takes place primarily at the active centers on the lichen biomass's surface, and that subsequent diffusion into the pores of the lichen biomass has gradually occurred. When the two models are evaluated together, velocity on biosorption of SO on to the lichen biomass is determined by rapid diffusion of the surface with relatively slower particle diffusion. According to these results, the biosorption of SO onto the lichen biomass was controlled by chemisorption [50, 51].

Table 5 Comparison of the uptake capacities for SO dye of reported various adsorbents in the literature

Adsorbent	pH	Temperature/°C	Max. sorption capacity, /mol kg^{-1}	References
Coal fly ash	9	30	0.00503	[40]
CO_2 neutralized activated red mud	8.3	29	0.0278	[41]
Pineapple peels waste	–	30	0.0618	[42]
Alkali-treated mango seed	10	25	0.0884	[43]
Alkali-treated rice husk	–	35	0.0278	[44]
Sugarcane bagasse	10	25	0.168	[45]
Pineapple peel	6	25	0.0743	[46]
Kaolinite cay	–	31	0.0463	[47]
Evernia prunastri biomass	6	25	0.257	This study

3.6 Biosorption thermodynamics

In order to explain the thermodynamic behavior of SO biosorption onto lichen biomass, it was studied at temperatures of 5 °C, 25 °C, and 40 °C and Fig. 5 was obtained. Biosorption enthalpy was found positive. ΔH^0 was calculated as 27. 5 kJ mol^{-1} showed that the biosorption process was endothermic. ΔS^0 was calculated as 136 $Jmol^{-1}$ K^{-1}. This situation can be explained by the release of water molecules due to the electrostatic interaction between the SO and active center on the lichen biomass surface. This can be explained by the increase of irregularity in the solid/liquid interface [52]. The free energy value was found as − 10.3 kJ mol^{-1}, − 12.9 kJ mol^{-1}, and − 15.1 kJ mol^{-1} at 5 °C, 25 °C, and 40 °C, respectively. This result indicates that biosorption tends to occur spontaneously with increasing temperature [53]. The negative free energy value indicated that spontaneous biosorption was possible. The results of biosorption thermodynamics showed that the biosorption process was feasible, spontaneous, and endothermic. Moreover, the value of the DR model indicates that the biosorption is chemical. Also, kinetic results indicate that the biosorption is controlled by chemisorption. When this value is evaluated with the thermodynamic data, the biosorption process is chemical.

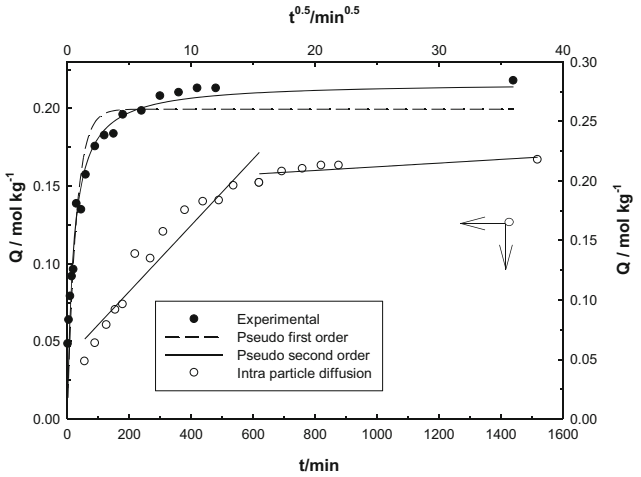

Fig. 4 Effect of contact time on biosorption of SO onto lichen ($[SO]_0$:500 mg L^{-1}, biosorbent dosage:300 mg, V:30 mL, pH:6.0, contact time:2–1440 min, temperature: 25 °C)

3.7 Biosorption-desorption performance

The re-use of biosorbent is very important to make the biosorption process more economical. Reusability investigated the desorption ability for SO onto lichen biomass. The *Evernia prunastri* biosorbent was regenerated using HCl, NaOH, and ethyl alcohol. The results were given in Fig. 6. According to the results of recovery experiments, the highest desorption capacity was examined with the HCl (51%) solution. The minimum recovery percentage for SO onto lichen biomass was achieved with ethyl alcohol (18%).

3.8 FT-IR, SEM-EDX, and BET analyses

The FT-IR analyses give major data about the characteristic peaks of the lichen biomass in the biosorption process. In the

Table 6 PFO, PSO, and IPD kinetic models parameters

Kinetic model	Parameter	Value	R^2
PFO	Q_t/mol kg^{-1}	0.218	0.906
	Q_e/mol kg^{-1}	0.200	
	$k_1 \times 10^3/dk^{-1}$	35.5	
	$Hx10^3$/mol kg^{-1} min^{-1}	7.10	
PSO	Q_t/mol kg^{-1}	0.218	0.965
	Q_e/mol kg^{-1}	0.217	
	$k_2 \times 10^3/mol^{-1}kg$ min^{-1}	233	
	$Hx10^3$/mol kg^{-1} min^{-1}	10.9	
IPD	$k_i \times 10^3/molkg^{-1}$ $min^{-0.5}$	51.5	0.915

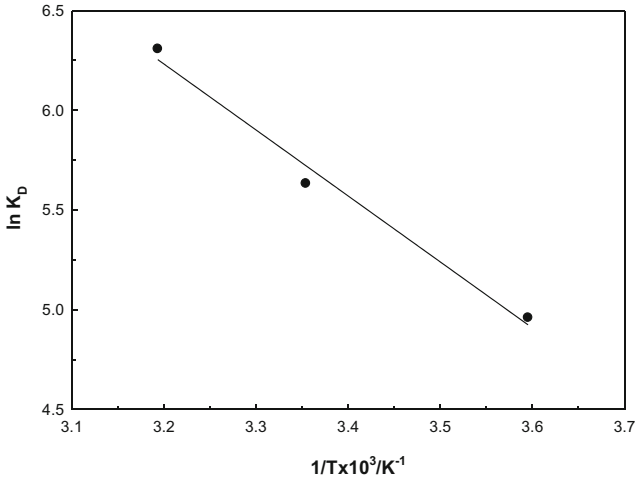

Fig. 5 Effect of temperature on biosorption of SO onto lichen ($[SO]_0$:500 mg L^{-1}, biosorbent dosage:100 mg, V:10 mL, pH:6.0, contact time:1440 min, temperature: 5 °C, 25 °C and 40 °C)

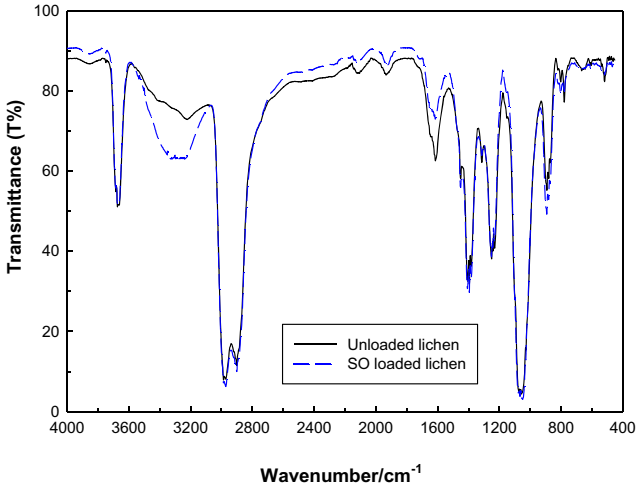

Fig. 7 FT-IR spectra of lichen biosorbent before and after biosorption of SO

current paper, the FT-IR analyses of lichen biomass before and after biosorption was done (Fig. 7). According to Fig. 7, lichen biomass has characteristic peaks. The strong bands at 3307 cm^{-1} were due to a bounded hydroxyl group (–OH) and amino ($-NH_2$) groups stretching vibrations on the surface of the lichen biomass. The peaks at 2896–2972 cm^{-1} were attributed to the C–H group. The peaks of the carboxyl group (−C=O) groups were observed at 1608 cm^{-1}. The bands observed at 1059 cm^{-1} was attributed to −C=O stretching of alcohols and carboxylic acids on the lichen [54, 55]. On the other hand, after the biosorption of SO, the bending vibrations and symmetric/asymmetric stretching vibrations of the characteristic peaks of $-NH_2$, −OH, and − C=O groups were shifted to 3250 cm^{-1}, 2985 cm^{-1}, 2872 cm^{-1}, 2985 cm^{-1}, 1530 cm^{-1}, and 1049 cm^{-1}, respectively. Previously, Giambattista [56] studied the details of the FT-IR and SEM analysis of *Evernia prunastri*, and reported that the region between 1800 and 1480 cm^{-1} was related with the Amide bands of proteins. And also, it was showed that the bands located at the 1722 cm^{-1} was revealed with C=O vibrations of polysaccharides found on the surface of the lichen [57]. It is considered that the functional groups of polysachharides and proteins were involved in the biosorption process. The attractions cationic SO dye and the surface groups of the lichen biomass could be carried out via complex formation.

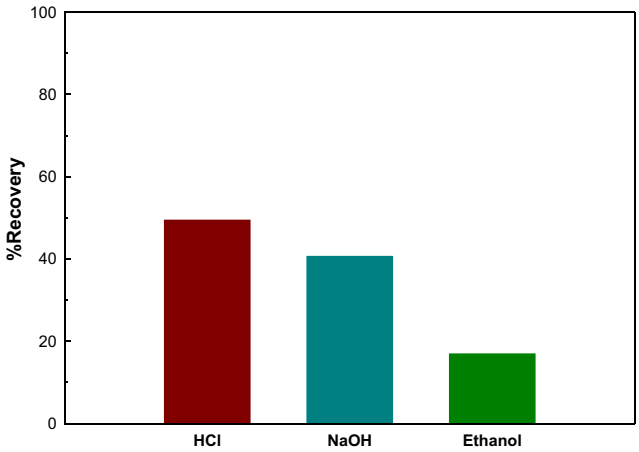

Fig. 6 Recovery percent for desorption of SO onto lichen ($[SO]_0$:500 mg L^{-1}, biosorbent dosage:100 mg, V:10 mL, pH:6.0, contact time:1440 min, temperature: 25 °C)

In order to define the surface morphology of the lichen biomass, before and after biosorption was taken from the samples. SEM images of lichen biosorbent, before and after SO biosorption, were shown in Fig. 8. SEM images of lichen biosorbent showed particles that are a huge porous with irregular shapes, rough, and edges. The surface of the lichen biomass after SO biosorption was largely rounded and smooth indicating that the particles deposited were SO. This view might be owing to the electrostatic interactions between SO with the active centers on the surface of the lichen biomass.

Figures 8c and d show the EDX results before and after SO biosorption on the lichen surface. According to the results of Fig. 8c, lichen consists of C, O, Al, Si, K, and Ca elements as well as substantially C and O. On the other hand, N and Cl elements (Fig. 8d) in the structure of the SO dye appeared in the EDX spectrum after biosorption supported SO biosorption by the lichen biomass. Changes in the stretching of functional groups belonging to lichen biomass after SO biosorption seen in the results of FT-IR analyses were related to the interaction of SO molecules with active centers in lichen biomass functional groups. Also, changes in SEM images after SO biosorption and EDX analysis results also prove SO biosorption onto the active sites of the lichen surface.

The surface area and pore size of *Evernia prunastri* biomass were determined by N_2 adsorption-desorption at

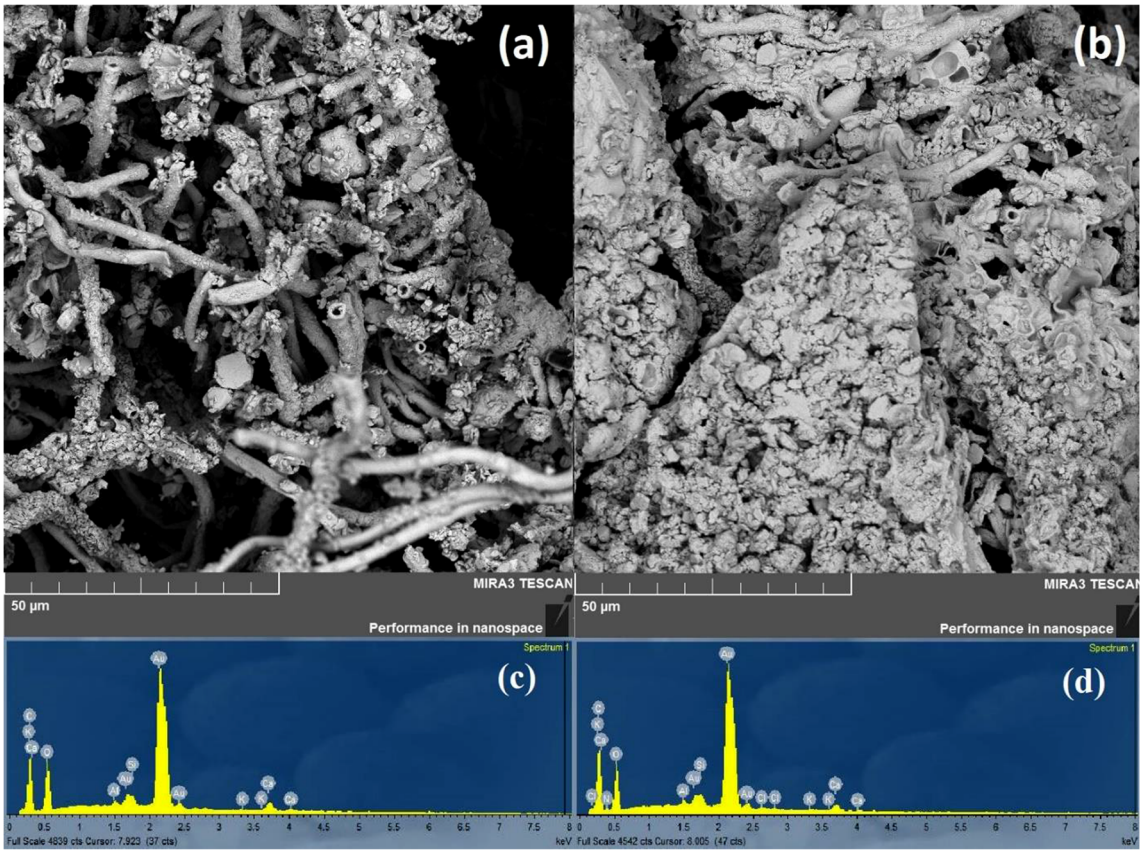

Fig. 8 SEM photographs of lichen (**a**) and SO biosorbed lichen (**b**) and EDX results of lichen before (**c**) and after (**d**) biosorption of SO

77 K. Nitrogen adsorption-desorption isotherms of lichen before and after SO biosorption, and the results of BET analysis were given in Fig. 9 and Table 7, respectively. The surface area of lichen biomass is 38.2 m^2 g^{-1} calculated by BET method. The pore size is mainly about 1.85 nm and the total pore volume of lichen biomass is 0.00681 cm^3 g^{-1}. According to IUPAC, if the pore diameter of the materials is in the range of 2–50 nm and > 50 nm, the mesopore and macropore are defined, respectively. On the other hand, if the pore diameter is < 2 nm, the structure is defined as microporous [58]. When Table 7 was examined, it is seen that the porous diameter of lichen was < 2 nm, which indicates that lichen has a microporous structure. When Fig. 9 is examined, it is observed that the difference between biosorption and desorption is small, indicating that the lichen has a microporous structure. Microporosity increased after SO biosorption (Table 7). This increase in the microporosity after SO biosorption was thought to be the result of the narrowing of the pores after biosorption.

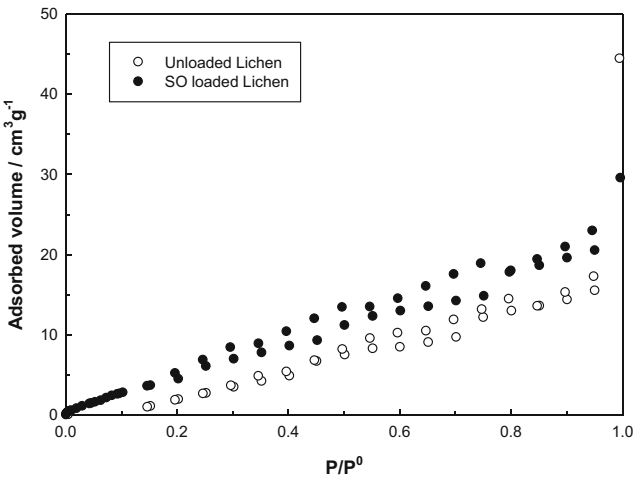

Fig. 9 Nitrogen biosorption-desorption isotherms of lichen before and after biosorption of SO. ($[SO]_0$:500 mg L^{-1}, biosorbent dosage:100 mg, V:10 mL, pH:6.0, contact time:1440 min, temperature: 25 °C)

4 Conclusion

The lichen biomass was used effectively as biosorbent for the cationic dye SO removal from aqueous solution. FT-IR, SEM-EDX, and BET analysis results showed that SO biosorbed onto the lichen biomass. All parameters affecting the removal of SO from aqueous solution were investigated and optimal conditions were determined in detail. Optimal study conditions for maximum biosorption efficiency were determined.

Table 7 Changes in specific surface area and pore characteristics of Lichen before and after biosorption of SO

Sample	S_{BET}[a] (m^2 g^{-1})	V_{Total}[b] (cm^3 g^{-1})	V_{micro}[c] (cm^3 g^{-1})	Dp (Å)
Lichen	38.2	0.0813	0.00681	17.5
Lichen-SO	45.5	0.0564	0.01441	11.0

[a] Multipoint BET method

[b] Volume adsorbed at $p/p0 = 0.99$

[c] Micropore volume calculated by DR method

The pH of the solution was optimally adopted as pH:6.0 for maximum and stable biosorption, and the amount of bisorbent, the contact time and the temperature were found to be 100 mg, 1440 min, 25 °C, respectively. Under optimal conditions, the maximum biosorption capacity was calculated as 0.257 mol kg^{-1}. The biosorption energy for SO onto the lichen biomass which was found to be $E_{DR:}$8.9 kJ mol^{-1} reveals the biosorption proceeds chemically. The biosorption process follows the PSO and IPD model kinetics. Thermodynamic parameters indicated that biosorption process was endothermic, possible, and spontaneous. All obtained results showed that the *Evernia prunastri* biomass can be effectively used as biosorbent with easy and economic preparation, environmentally friendly, thermodynamically favorable, and high biosorption capacity with the purpose of removal of the cationic SO dye from the wastewater.

Funding The present study was partly supported by the Cumhuriyet University Scientific Research Projects Commission (CUBAP), Sivas in Turkey.

Compliance with ethical standards

Conflict of interest The authors declare that they have no conflict of interest.

References

1. Güvenç Ş, Bilgin A, Bayrak K, Yümün ZÜ, Kam E, Yasemin S, Karaca M (2018) Which is the better as an indicator of environmental quality: *Parmelia sulcata* Taylor or Parmelina tiliacea (Hoffm) Hale. J Biol Environ Sci 12(34):1–6
2. Rai AN (1988) Nitrogen metabolism. In: Galun M (ed) CRC handbook of lichenology, vol I. CRC Press, Boca Raton, pp 201–237
3. Nash TH (ed) (1996) Lichen biology. Cambridge University Press
4. Aslan A, Yazici K (2006) Contribution to the lichen flora of Giresun province of Turkey. Acta Bot Hungar 48(3–4):231–245
5. Hale ME, Ocampo-Friedmann R (1984) Ascospore cultures of lichen phycobionts from the Antarctic desert. Antarct J US 19:170
6. Sanders WB, de Los RA (2019) Structural evidence of diffuse growth and parenchymatous cell division in the cortex of the umbilicate lichen Lasallia pustulata-erratum. Lichenologist 51(4):393–393
7. Karunaratne DN, Jayalal RGU, Karunaratne V (2012) Lichen polysaccharides. The complex world of polysaccharides, pp 215-226
8. Gül ÜD, Şenol ZM, Gürsoy N, Şimşek S (2019) Effective UO_2^{2+} removal from aqueous solutions using lichen biomass as a natural and low-cost biosorbent. J Environ Radioact 205:93–100
9. Bayazıt G, Gül ÜD, Ünal D (2018) Biosorption of Acid Red P-2BX by lichens as low-cost biosorbents. Int J Environ Sci 76(4):608–615
10. Şenol ZM, Gül ÜD, Şimşek S (2019) Assessment of Pb^{2+} removal capacity of lichen (*Evernia prunastri*): application of adsorption kinetic isotherm models and thermodynamics. Environ Sci Pollut Res 26(26):27002–27013
11. Shibata S (1973) Some recent studies on the metabolites of fungi and lichens. Pure Appl Chem 33(1):109–128
12. Marahel F, Ali Khan M, Marahel E (2015) Kinetics thermodynamics and isotherm studies for the adsorption of BR2 dye onto avocado integument. Desalin Water Treat 53(1):826–835
13. Korbahti BK, Rauf MA (2008) Application of response surface analysis to the photolytic degradation of basic Red 2 dye. Chem Eng J 138(1):166–171
14. Anitha T, Senthil Kumar P, Sathish Kumar K (2016) Synthesis of nano-sized chitosan blended polyvinyl alcohol for the removal of Eosin Yellow dye from aqueous solution. J Water Process Eng 13: 127–136
15. Tharaneedhar V, Kumar PS, Saravanan A, Ravikumar C, Jaikumar V (2017) Prediction and interpretation of adsorption parameters for the sequestration of methylene blue dye from aqueous solution using microwave assisted corncob activated carbon. Sustain Mater Technol 11:1–11
16. Shah K, Parmar A (2018) Removal of Safranin O dye from synthetic wastewater by Activated Carbon prepared from Tamarind seeds. Int J Appl Eng Res 13(11):10105–10107
17. Ponnusamy SK, Subramaniam R (2013) Process optimization studies of Congo red dye adsorption onto cashew nut shell using response surface methodology. Int J Ind Chem 4:17
18. Kumar PS, Varjani SJ, Suganya S (2018) Treatment of dye wastewater using an ultrasonic aided nanoparticle stacked activated carbon: kinetic and isotherm modelling. Bioresour Technol 250:716–722
19. Rajkumar P, Senthil Kumar P, Dinesh Kirupha S, Vidhyadevi T, Nandagopal J, Sivanesan S (2013) Adsorption of Pb (II) ions onto surface modified *Guazuma ulmifolia* seeds and batch adsorber design. Environ Prog Sustain 32:307–316
20. Senthil Kumar P, Sivaranjanee R, Vinothini U, Raghavi M, Rajasekar K, Ramakrishnan K (2014) Adsorption of dye onto raw and surface modified tamarind seeds: isotherms, process design, kinetics and mechanism. Desalin Water Treat 52:2620–2633
21. Kumar PS, Abhinaya RV, Lashmi KG, Arthi V, Pavithra R, Sathyaselvabala V, Sivanesan S (2011) Adsorption of methylene blue dye from aqueous solution by agricultural waste: equilibrium, thermodynamics, kinetics, mechanism and process design. J Colloid 73:651
22. Senthil Kumar P, Fernando PSA, Ahmed RT, Srinath R, Priyadharshini M, Vignesh AM, Thanjiappan A (2014) Effect of temperature on the adsorption of methylene blue dye onto sulfuric acid–treated orange peel. Chem Eng Commun 201:1526–1547

23. Suganya S, Saravanan A, Ravikumar C (2017) Computation of adsorption parameters for the removal of dye from wastewater by microwave assisted sawdust: theoretical and experimental analysis. Environ Toxicol Pharmacol 50:45–57
24. Pavithra KG, Jaikumar V (2019) Removal of colorants from wastewater: a review on sources and treatment strategies. J Ind Eng Chem 75:1–19
25. Bayazıt G, Tastan BE, Gül ÜD (2019) Biosorption isotherm and kinetic properties of common textile dye by Phormidium animale. Global Nest J 21:1–7
26. El-Moselhy MM, Ates A, Çelebi A (2017) Synthesis and characterization of hybrid iron oxide silicates for selective removal of arsenic oxyanions from contaminated water. J Colloid Interface Sci 488:335–347
27. Shariati S, Faraji M, Yamini Y, Rajabi AA (2011) Fe_3O_4 magnetic nanoparticles modified with sodium dodecyl sulfate for removal of safranin O dye from aqueous solutions. Desalination 270(1–3): 160–165
28. Langmuir J (1918) The adsorption of gases on plane surfaces of glass mica and platinum I. J Am Chem Soc 40:1361–1403
29. Freundlich H, Heller W (1939) The adsorption of cis- and transazobenzene. J Am Chem Soc 61:2228–2230
30. Dubinin MM, Zaverina ED, Radushkevich LV (1947) Sorption and structure of active carbons I Adsorption of organic vapors. Russ J Phys Chem A 21:1351–1362
31. Sivakumara D, Parthibanb R, Kumarb PS, Saravananc A (2020) Synthesis and characterization of ultrasonic-assisted *Delonix regia* seeds: modelling and application in dye adsorption. Desalin Water Treat 173:427–441
32. Ho YS (2006) Pseudo-second-order model for lead ion sorption from aqueous solutions onto palm kernel fiber. J Hazard Mater: 129–137
33. Jothirani R, Kumar PS, Saravanan A, Narayan AS, Dutta A (2016) Ultrasonic modified corn pith for the sequestration of dye from aqueous solution. J Ind Eng Chem 39:162–175
34. Joulain D, Tabacchi R (2009) Lichen extracts as raw materials in perfumery. Part 1: Oakmoss. Flavour Frag J 24(2):49–61
35. Karunaratne DN, Jayalal RGU, Karunaratne V (2012). Lichen polysaccharides. The complex world of polysaccharides, pp 215–226
36. Takeda T, Funatsu M, Shibata S, Fukuoka F (1972) Polysaccharides of lichens and fungi V Antitumor active polysaccharides of Evernia pacroscyphus and Alectoria species. Chem Pharm Bull 20:2445–2454
37. Şenol ZM (2020) Effective biosorption of Allura red dye from aqueous solutions by the dried-lichen (Pseudoevernia furfuracea) biomass. Int J Envıron An Ch:1–15
38. Bağcı S, Ceyhan A (2015) Adsorption of methylene blue onto activated carbon prepared from *Lupinus albus*. Chem Ind Chem Eng Q 22:30–30
39. Sadaf S, Bhatti HN (2014) Batch and fixed bed column studies for the removal of Indosol Yellow BG dye by peanut husk. J Taiwan Inst Chem Eng 45:541–553
40. Dwivedi MK, Jain N, Sharma P, Alawa C (2015) Adsorption of safranin from wastewater using coal fly ash. IOSR-JAC 8(4):27–35
41. Sahu MK, Sahu UK, Patel RK (2015) Adsorption of safranin-O dye on CO_2 neutralized activated red mud waste: process modelling, analysis and optimization using statistical design. RSC Adv 5(53): 42294–42304
42. Mohammed MA, Ibrahim A, Shitu A (2014) Batch removal of hazardous safranin-O in wastewater using pineapple peels as an agricultural waste based adsorbent. J Environ Monit 2(3):128–133
43. Malekbala MR, Soltani SM, Yazdi SK, Hosseini S (2012) Equilibrium and kinetic studies of safranine adsorption on alkali-treated mango seed integuments. Int J Chem Eng Appl 3(3):160–166
44. Chowdhury S, Misra R, Kushwaha P, Das P (2011) Optimum sorption isotherm by linear and nonlinear methods for safranin onto alkali-treated rice husk. Bioremediat J 15(2):77–89
45. Farahani M, Kashisaz M, Abdullah SRS (2015) Adsorption of safranin O from aqueous phase using sugarcane bagasse. Int J Ecol Sci Environ Eng 2:17–29
46. Yusuf M, Elfghi FM, Mallak SK (2015) Kinetic studies of safranin-O removal from aqueous solutions using pineapple peels. Iran J Energy Environ 6(3):173–180
47. Adebowale KO, Olu-Owolabi BI, Chigbundu EC (2014) Removal of safranin-O from aqueous solution by adsorption onto kaolinite clay. J Encap Ads Sci 4(03):89
48. Kumar PS, Pavithra J, Suriya S, Ramesh M, Kumar KA (2015) Sargassum wightii, a marine alga is the source for the production of algal oil, bio-oil, and application in the dye wastewater treatment. Desalin Water Treat 55:1342–1358
49. Yaashikaa PR, Kumar PS, Varjani SJ, Saravanan A (2019) Advances in production and application of biochar from lignocellulosic feedstocks for remediation of environmental pollutants. Bioresour Technol 292:122030
50. Ahmad AA, Hameed BH, Aziz N (2007) Adsorption of direct dye on palm ash: kinetic and equilibrium modeling. J Hazard Mater 141(1):70–76
51. Kaveeshwar AR, Ponnusamy SK, Revellame ED, Gang DD, Zappi ME, Subramaniam R (2018) Pecan shell based activated carbon for removal of iron(II) from fracking wastewater: adsorption kinetics isotherm and thermodynamic studies. Process Safe Environ 114: 107–122
52. Şimşek S, Şenol ZM, Ulusoy HI (2017) Synthesis and characterization of a composite polymeric material including chelating agent for adsorption of uranyl ions. J Hazard Mater 338:437–446
53. Ai T, Jiang X, Liu Q, Lv L, Wu H (2019) Daptomycin adsorption on magnetic ultra-fine wood-based biochars from water: kinetics isotherms and mechanism studies. Bioresour Technol 273:8–15
54. Ekmekyapar F, Aslan A, Bayhan YK, Cakici A (2006) Biosorption of copper(II) by nonliving lichen biomass of Cladonia rangiformis hoffm. J Hazard Mater 137(1):293–298
55. Uluozlu OD, Sarı A, Tuzen M, Soylak M (2008) Biosorption of Pb(II) and Cr(III) from aqueous solution by lichen (Parmelina tiliaceae) biomass. Bioresour Technol 99(8):2972–2980
56. Giambattista LD, Grimaldi P, Gaudenzi S, Pozzi D, Grandi M, Morrone S, Silvestri I, Congiu Castellano A (2010) UVB radiation induced eVects on cells studied by FTIR spectroscopy. Eur Biophys J 39:929–934
57. Gurbanov R, Unal D (2018) The biomolecular alterations in cladoniaconvoluta in response to lead exposure. Spectrosc Lett 51:563–570
58. Kumari P, Sharma P, Srivastava S, Srivastava MM (2006) Biosorption studies on shelled Moringa oleifera Lamarck seed powder: removal and recovery of arsenic from aqueous system. Int J Miner Process 78:131–139